33RD CONGRESS
OF THE INTERNATIONAL COUNCIL
OF THE AERONAUTICAL SCIENCES
STOCKHOLM, SWEDEN, 4-9 SEPTEMBER, 2022

ZONAL MODEL BASED AIRCRAFT PASSENGER THERMAL COMFORT COMPARATIVE STUDY

Sergi Tarroc Gil[1], Jörg Schminder[1], Alex Guerrero i Almirall[2], Jose Ignacio Tarraga Prieto[3] & Renato Vaz Linn[4]

[1]Linköping University
[2]UptimAI
[3]MAHLE Electronics S.L.U
[4]Federal University of Rio Grande do Sul

Abstract

Computational simulations have become during the last decades an essential tool to be used every day sooner in the design chain within the aerospace industry, leading to better decision making and more efficient concepts. However, in the aircraft design field, the thermal comfort of the passengers is not assessed until late design stages due to the complexity and high computational cost of simulating the flow inside it. The present work has the aim to show the Zonal Model approach as a solid early design simulation alternative to conventional CFD. A complete Fractional Step based Zonal Model solver is proposed, able to provide first estimations to the two-dimensional fluid solution, for a given cabin concept, with a low computational cost associated. This solver has also integrated its own automatized mesh generation algorithm along with a Radial Basis Functions morphing tool. With this method, a set of comparative studies have been performed for comparing several cabin design parameters attending to the thermal comfort of passengers and crew, giving a demonstration of the capabilities that this Zonal Model approach has for early aircraft design optimization and decision making.

Keywords: Zonal Model, Thermal Comfort, Fluid Simulation and Aircraft Cabin Design.

1. Introduction

The aviation industry is at the beginning of a historic transformation away from climate-damaging towards climate-neutral aviation. Hybrid and all-electric aircraft are design solutions of the future. However, these new concepts also come with new technical challenges. One of these is the thermal management of all onboard electronic power units, equipment, and cabin air conditioning. A good understanding of the thermal processes is particularly important for achieving a high level of thermal comfort for the crew and passengers. The interaction of the thermal aspects of different aircraft systems can already be determined in the preliminary design phase using 1D simulation models. Nevertheless, thermal comfort design issues are still addressed relatively late in the aircraft development process when the basic aircraft design has already been defined. This has two clear disadvantages: on the one hand, necessary changes in the aircraft design can lead to project delays and high costs and, on the other hand, the cost-intensive CFD simulations typically used in detailed design phases only allow small improvements at the level of detail but not extensive optimizations as they are common during the preliminary design phase searching for the concept that best meets the requirements.

In order to carry out thermal comfort studies and optimizations as early as the conceptual design phase, a faster numerical simulation strategy is required which at the same time does not oversimplify the complex relationships between cabin air ventilation and occupants' thermal perception. One approach to get closer to this goal is the use of a Zonal Model, a fluid simulation approach that has been traditionally used for evaluation of indoor circulation in buildings [12] [19], but also has some first research experiences for assessing the thermal comfort in aircraft cabins with promising results [7][2][18]. In this simulation technique, the aircraft cabin is divided into several sub-zones in which the flow and heat transport phenomena are evaluated. In contrast to classic CFD simulations, the thermo-physical variables are calculated on a much coarser mesh (in the order of $10^1 - 10^2$ zones or elements), which results in a significant increase in the speed of the solution, but also in a reduction of accuracy. Yet, the Zonal Model approach maps the relevant macroscopic effects for assessing the thermal comfort, such as temperature distribution and velocity field, providing much more information than single-node models.

In this paper, the Zonal Model developed in [18] is extended for performing comparative studies for assessing the convenience of several cabin design concepts attending to the thermal comfort of the passengers and crew. The current method consists of a two-dimensional Zonal Model solver with its own integrated automatic mesh generation and morphing framework. The present work aims to show the reliability of Zonal Model analyses, their computational feasibility and the capabilities of this approach for sensibly improving the resulting cabin design concepts.

2. Method

First, the cabin geometry is defined, in a CAD software, as a set of two-dimensional closed NURBS curves representing the contour of a cabin section and importing them to the algorithm as an IGES file [15]. Then, setting the element size along with other parameters, the algorithm generates a two-dimensional unstructured mesh of QUAD and TRIA elements through a grid-based methodology [10][9]. For meshing, the domain defining NURBS are discretized in segments that are afterwards intersected with a regular background mesh, solving the boundary elements through a set of templates. For improving the quality of the result some node catching routines are included as well as an iterative Laplacian smoothing method once the mesh is solved. The computation time for generating a mesh in the Zonal Model range for a laptop with an Intel® Core™ i5-6200U CPU @ 2.30GHz processor is below 10 s (see Figure 1a).

The developed algorithm also includes a Radial Basis Functions (RBS) morphing tool [5] for adapting an already existing mesh to a new geometry. This method for generating new meshes from a previous one reduces the computation time and improves its scalability (see Figure 1a). However, this improvement does not have a significant impact on the typically reduced amount of elements of a Zonal Model approach. Instead, this is especially useful for comparative analysis in which morphologically similar cabin geometries are studied, reducing the human task and its associated possible errors. Additionally, the results for a base mesh can be directly used as initial conditions for derived morphed meshes, which can reduce drastically the time for converging the solution.

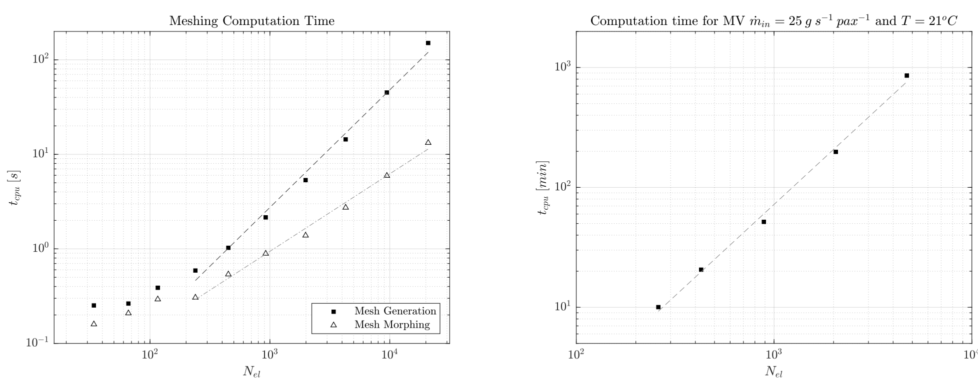

(a) Meshing and Morphing routines. (b) Solver for the reference cabin case.

Figure 1 – Computation time for the meshing and morphing algorithm and the Zonal Model solver.

The fluid solver consists of a two-dimensional incompressible Fractional Step solver for co-located meshes, with a Boussinesq term for considering the natural convection effects. Numerically, the solver contains an explicit Rhie and Chow term [14][16] on the mass flow evaluation, cross-diffusion corrections [11], and a set of High-Resolution Schemes (HRS) [17] eligible by the user. The convergence is evaluated in the time-averaged fields since the ventilation solution uses to be a statistically stationary condition. This Fractional Step Zonal Model solver has been already validated by Tarroc [18] with Differential Heated Cavity, Driven Cavity and Inlet Cases. The computation time required for a laptop, with an Intel® Core™ i5-6200U CPU @ 2.30GHz processor, to converge the solution of the reference cabin case is shown in Figure 1b (narrow-body cabin of Figure 3a). Note that the time required to solve the problem for Zonal Model sized meshes (i.e. in the order of 10^2 elements) is in the order of 10 min, being feasible to run a set of several cases, for comparative studies, in a reasonable amount of time. Although the results are not accurate on the small scales, the solver has shown to correctly represent macroscopic effects and trends, being this representative for having rough estimations and performing comparative assessments.

Once the flow is solved, the thermal comfort of the passengers is assessed through the thermal comfort parameters defined in ISO7730:2005 [8], and evaluated in a set of Detective Points around the passengers – 5 cm away from them [13] (see Figure 3a). These parameters, or objective functions, evaluate the percentage of dissatisfied passengers relaying in empirical correlations obtained by exposing a significant sample of people to diverse ambient conditions with different levels of physical activity and clothing. Thermal dissatisfaction can be caused by different effects and the most relevant for this application are assessed in this paper:

- Predicted Percentage of Dissatisfied (PPD): general thermal comfort parameter derived from the Predicted Mean Vote (PMV) empirical index. This is dependent on the metabolic rate, the clothing and the air temperature, velocity, humidity and radiant temperature.
- Draught Rate (DR): percentage of dissatisfaction due to an excessive air current. This parameter is dependent on the air temperature, average velocity and turbulence intensity.
- Vertical Temperature Differential (PDver): percentage or dissatisfaction because of an excessive vertical temperature gradient from head to feet. This parameter is only dependent on the temperature spatial distribution.

Based on this thermal comfort evaluation methodology, comparative analyses can be done by simulating a set of cabins, modifying the desired design parameter and assessing the improvement in the objective function values obtained. Some of the possible parameters to modify are the inlet mass flow, the inlet temperature, the ventilation configuration (see Figure 2) or even the cabin geometry.

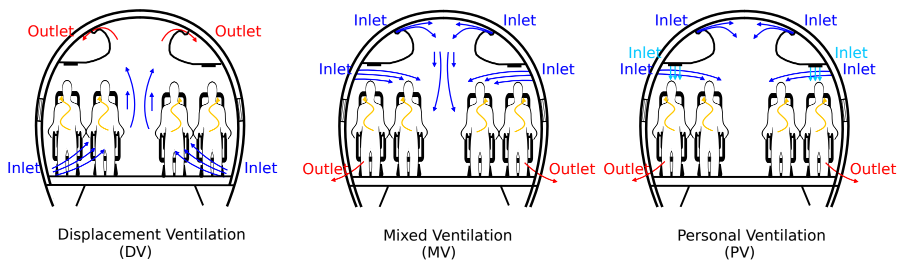

Figure 2 – Cabin ventilation configurations.

As a reference cabin, a narrow-body 2-2 seats configuration design, similar to the one studied by Raina et al. [1], is used. Its geometry is shown in Figure 3a, along with relevant data sampling locations. This reference cabin is discretized in 3 different Zonal Model meshes shown in Figures 3b, 3c and 3d along with their properties presented in Table 1.

Table 1 – Reference cabin meshes properties.

Mesh name	**Element size** $dx\ [cm]$	**Number of elements** N_{el}
msh10	10	243
msh06	6	645
msh03	3	2495

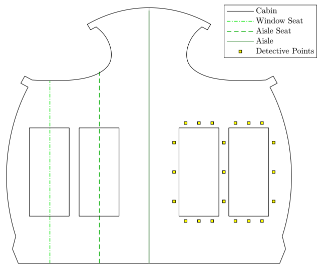

(a) Reference cabin geometry.

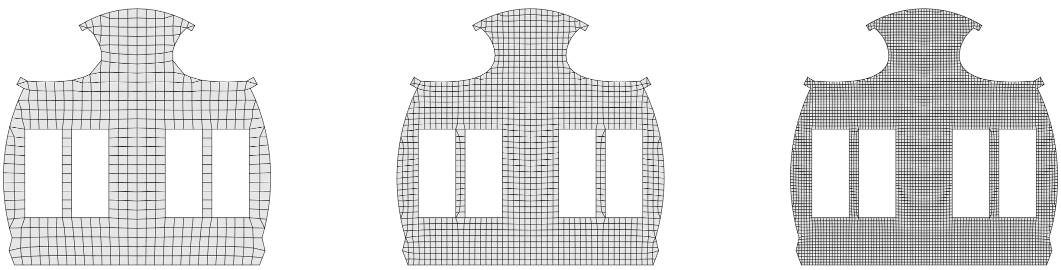

(b) Mesh *'msh10'*. (c) Mesh *'msh06'*. (d) Mesh *'msh03'*.

Figure 3 – Reference cabin geometrical design and Zonal Model meshes generated.

Afterwards, this study is extended for comparing the thermal performance response to changes in the cabin geometry. For doing it, 3 different narrow-body 2-2 seats layout aircraft cabin geometries are assessed under the same inlet conditions: MV configuration with an inlet temperature of $19^{o}C$. The assessed cabins shown in Figures 4a, 4b and 4c, from now on Cabin 1, 2 and 3, are respectively based on the cabin designs of Embraer 190 [6], de Haviland DASH 8 SERIES 100 [4] and ATR 42-30 [3]. Additionally, and with the aim to show the capabilities of this tool, Cabin 2 and 3 are morphed from the Cabin 1 mesh. The obtained meshes are shown in Figures 4d, 4e and 4f as well as their properties are presented in Table 2. Note that this study only replicates the geometry of the commercial cabins referenced, the ventilation layout and conditions are adapted to be equivalent for all the cases. Therefore, this is not a comparison between the performance of these commercial designs but a study of different cabin geometries under the same ventilation conditions.

Table 2 – Cabin 1, 2 and 3 mesh properties.

Mesh name	**Element size** $dx\ [cm]$	**Number of elements** N_{el}
Cabin 1 mesh	8	217
Cabin 2 mesh	8	217
Cabin 3 mesh	8	217

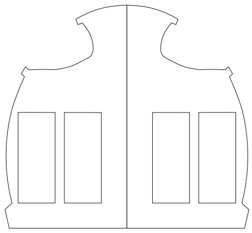

(a) Cabin 1 geometry and base for the morphing [6].

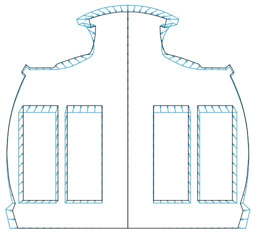

(b) Cabin 2 geometry and morphing field [4].

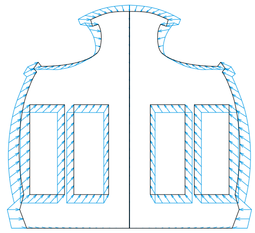

(c) Cabin 3 geometry and morphing field [3].

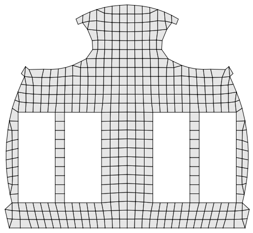

(d) Cabin 1 mesh.

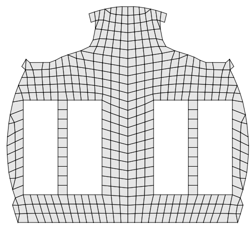

(e) Cabin 2 morphed mesh.

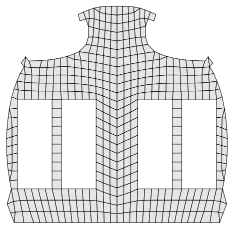

(f) Cabin 3 morphed mesh.

Figure 4 – Commercial aircraft based cabin geometries, morphing and meshes.

For all these studies, metabolic energy production (MET), basic clothing insulation (CLO), mean radiant temperature (TR) and relative humidity (RH) are parameters that are treated as constants in the PMV evaluation as in Pang et al. [13]. Additionally, 4 seated passengers are considered, represented as a constant energy source of 90 W each.

Table 3 – Fixed PMV parameters.

CLO $[clo]$	**MET** $[met]$	**TR** $[^{\circ}C]$	**RH** $[\%]$
0.90	1.12	21	30

3. Results

First, a mesh refinement study is performed for verifying the proper convergence of the velocity and temperature profiles for the reference cabin design presented in Figure 3a with a mixed ventilation configuration (MV), a inlet mass flow per passenger of $\dot{m}_{in} = 25\ g\, s^{-1}\ pax^{-1}$ and an inlet temperature of $T_{in} = 19^{o}C$ (see Figures 5a and 5b). This case is similar to the CFD analysis presented by Raina et al. [1], which serves as a reference for assessing the results obtained.

Afterwards, with the aim to show the capabilities of this methodology, design parameters comparatives are performed for the reference cabin with the mesh *msh10* (see Figure 3). For it, the objective functions are evaluated for a range of inlet mass flows, varying the ventilation configuration (Figure 6) and the inlet temperature (Figure 7). Finally, this inlet mass flow sweep is also studied for each of the 3 cabin geometries based on commercial aircrafts presented in Figure 4. The results of the cabin geometry comparative are shown in Figure 8. For each of the studies, The worst value of the objective functions captured at the detective points is plotted.

Additionally, the temperature and velocity fields are plot for significative data points of the ventilation configuration comparative (see Figure 9) and of the inlet temperature comparative (see Figure 10). The assessment of these fields is useful to understand the physical phenomena that is governing the behaviour of the objective functions shown in Figures 6 and 7 respectively.

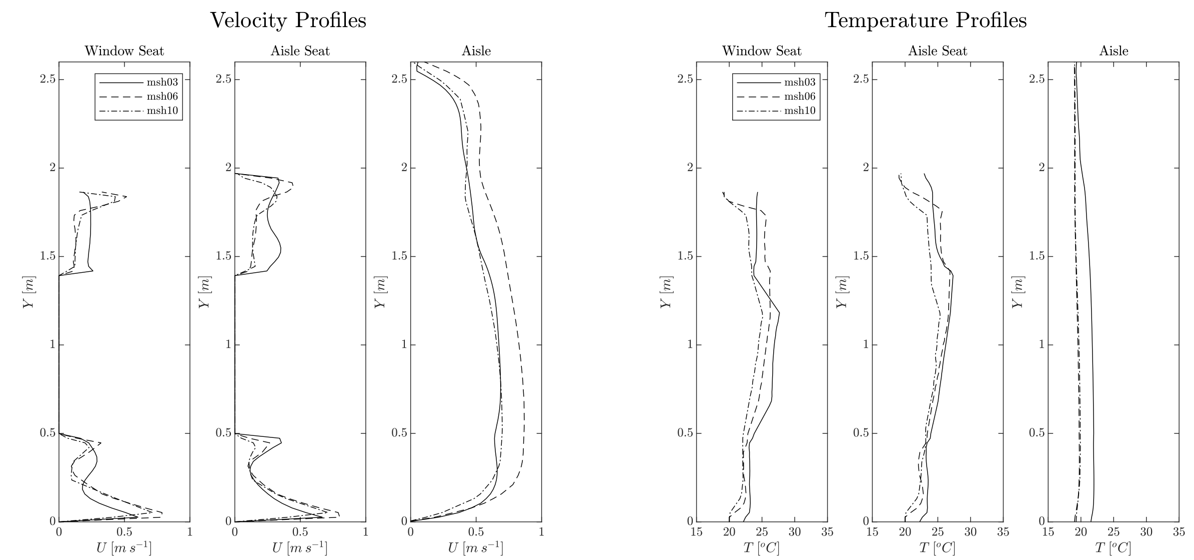

(a) Velocity profiles.

(b) Temperature profiles.

Figure 5 – Velocity and temperature profiles across the three representative sections for the mesh refinement study in the reference cabin.

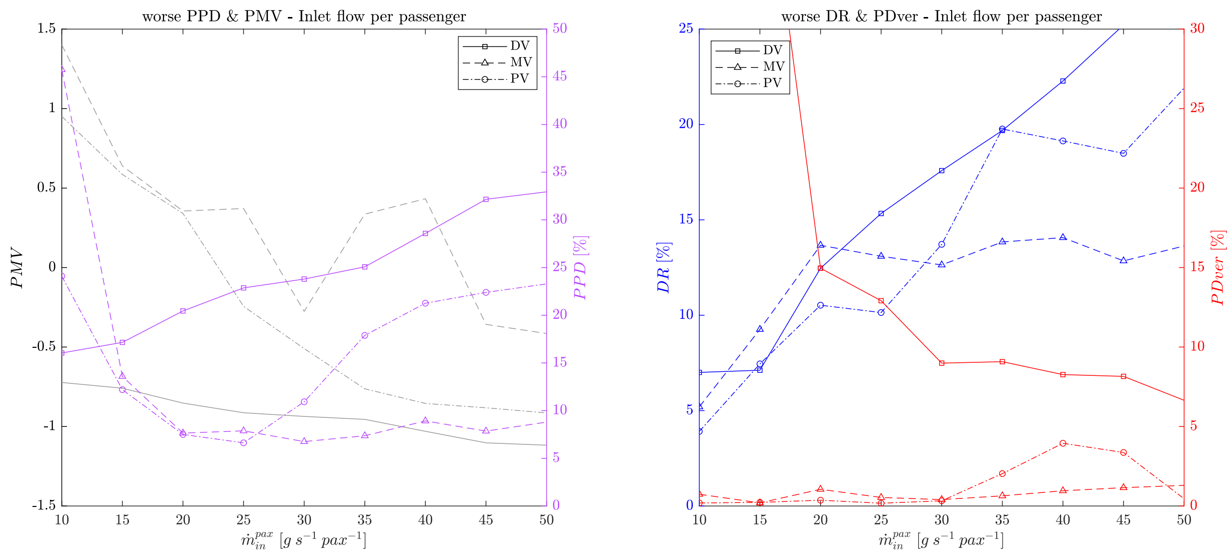

(a) PMV and PPV.

(b) DR and PDver.

Figure 6 – Objective functions for different ventilation configurations and inlet mass flows in the reference cabin. Fixed inlet temperature to $T_{in} = 19\,^{o}C$.

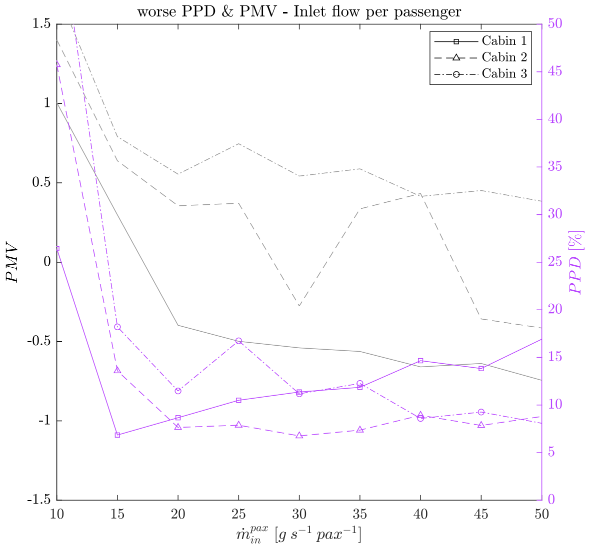

(a) PMV and PPV.

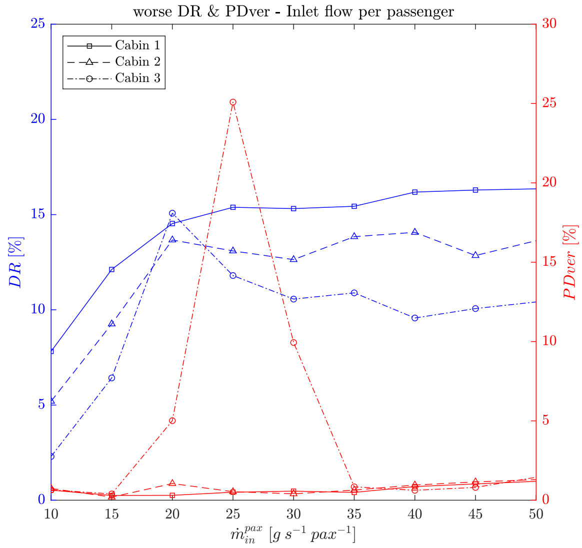

(b) DR and PDver.

Figure 7 – Objective functions for different inlet temperatures and mass flows in the reference cabin. Fixed ventilation configuration to MV.

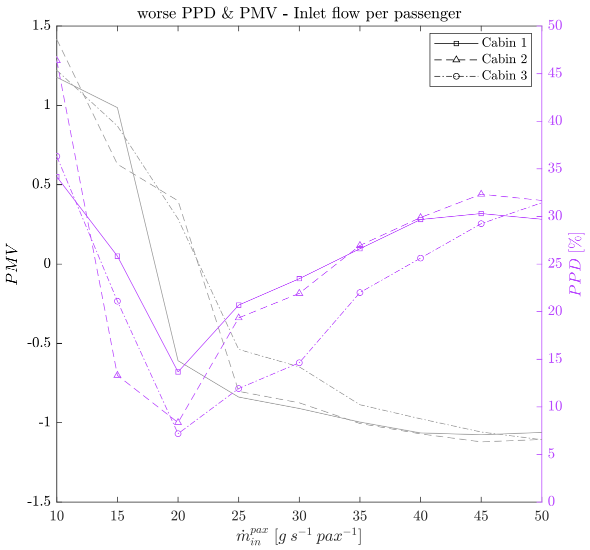

(a) PMV and PPV.

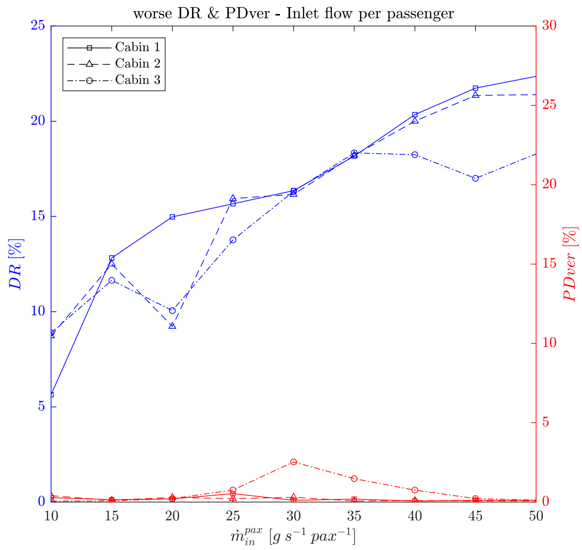

(b) DR and PDver.

Figure 8 – Objective functions for different cabin geometries and inlet mass flows. Fixed ventilation configuration to MV and inlet temperature to $T_{in} = 19\,^oC$.

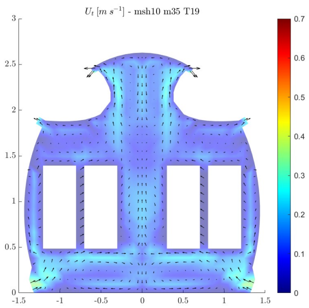

(a) Velocity field for DV configuration.

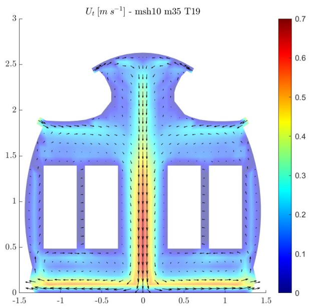

(b) Velocity field for MV configuration.

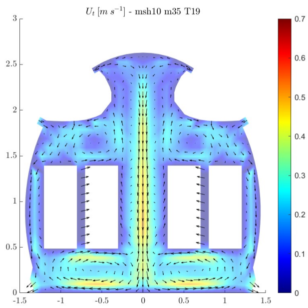

(c) Velocity field for PV configuration.

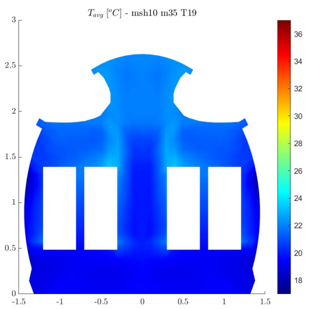

(d) Temperature field for DV configuration.

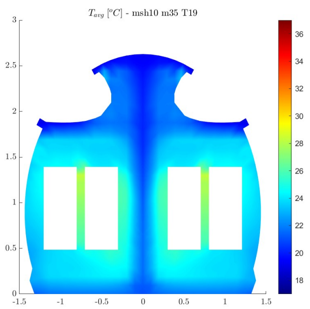

(e) Temperature field for MV configuration.

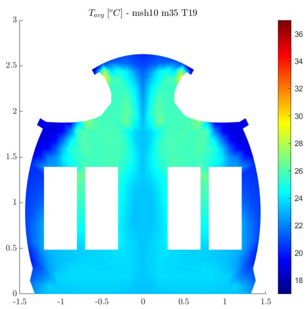

(f) Temperature field for PV configuration.

Figure 9 – Velocity and temperature fields for the ventilation configuration comparative in the reference cabin at $T_{in} = 19^oC$ and $\dot{m}_{in} = 35\,g\,s^{-1}\,pax^{-1}$.

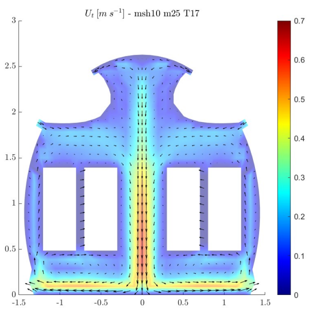

(a) Velocity field for $T_{in} = 17^oC$.

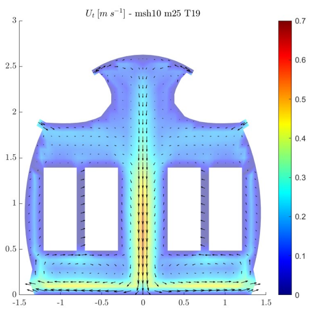

(b) Velocity field for $T_{in} = 19^oC$.

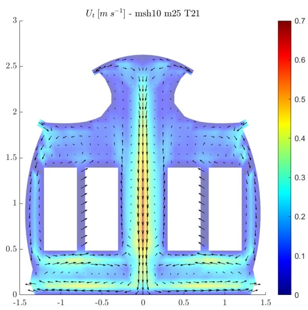

(c) Velocity field for $T_{in} = 21^oC$.

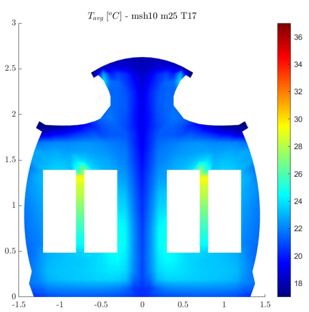

(d) Temperature field for $T_{in} = 17^oC$.

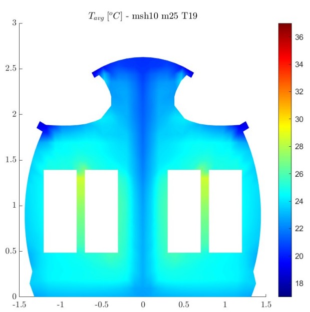

(e) Temperature field for $T_{in} = 19^oC$.

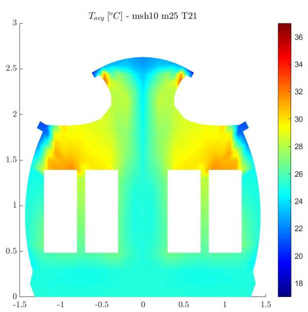

(f) Temperature field for $T_{in} = 21^oC$.

Figure 10 – Velocity and temperature fields for the inlet temperature comparative in the reference cabin for MV configuration and $\dot{m}_{in} = 25\,g\,s^{-1}\,pax^{-1}$.

4. Discussion

The results of the refinement verification study presented in Figures 5a and 5b show an adequate convergence of the velocity and temperature profiles in the three representative sections. Moreover, the profiles obtained are qualitatively similar to the ones presented by Raina et al. [1], sharing some velocity and temperature distribution patterns, despite not being the exact same case. It can also be seen from the results that, when refining the mesh, some local phenomena, not captured by the coarser meshes, arise. However, the results for the coarsest mesh are able to characterize the general behaviour of the flow, being this the aim of the Zonal Model approach, deeming *'msh10'* appropriate for computing the comparative studies.

Secondly, concerning the ventilation configuration comparative presented in Figure 6 some relevant observations can be done. The DV configuration shows an adequate performance for low inlet velocities when referring to PPV and DR, but an unacceptable vertical temperature gradient (PDver). In these conditions, the system is capable to evacuate the heat generated by the passengers with a low-velocity stream, but it does it stagnating the cold air at the bottom and the warm air on top. This configuration is able to generate a more uniform temperature distribution when increasing the inflow, reducing the PDver, but it is at the expense of having fast air streams close to the passengers (see Figure 9), leading to excessive PPD and DR values. On the contrary, MV and PV are very capable to maintain uniform temperature distributions around the passengers in all the studied range, as can be seen from their PDver parameter. It is also noticeable that while MV consistently shows good results in all the parameters for $\dot{m}_{in} \geq 20\, g\, s^{-1}\, pax^{-1}$, PV has an optimal performance in the range $15\, g\, s^{-1}\, pax^{-1} \geq \dot{m}_{in} \geq 30\, g\, s^{-1}\, pax^{-1}$ and the the results get worse for higher inlet values. This is explained because of the formation of recirculations over and beneath the passengers, inducing higher velocities around them and leading to a higher discomfort (see Figure 9). However, although the PV can lead to an unsatisfactory draught sensation under some conditions, it has to be also noted that the passengers will be able to modify the intensity of this inlet and eventually its direction, having an active control on the climatization and, thus, of their comfort.

Thirdly, regarding the inlet temperature comparative (see Figure 7), it can be observed that for low-temperature inlet ($T_{in} = 17^oC$) the optimal operation is found for low mass inflow, while the opposite happens for higher inlet temperature values ($T_{in} = 21^oC$) that operate better for higher mass inflow. In between, the $T_{in} = 19^oC$ inlet shows a consistently adequate behaviour for $\dot{m}_{in} \geq 20\, g\, s^{-1}\, pax^{-1}$. When it comes to the draught sensation (DR), higher inlet temperatures lead to a more thermally comfortable scenario, being in general better a warmer stream than a cold one. Lastly, the inlet temperatures studied show a uniform temperature distribution, except for a significative peak of dissatisfaction for $T_{in} = 21^oC$ around $\dot{m}_{in} = 25\, g\, s^{-1}\, pax^{-1}$. This event can be also qualitatively seen in Figure 10. While for $T_{in} = 17^oC$ and 19^oC the temperature is uniformly distributed around the passengers, there is a clear temperature accumulation over the passengers for $T_{in} = 21^oC$. This has its explanation, similarly to the previous comparative, in the formation of recirculation over the passengers' heads. This structure deflects the cooling air stream to the wall and retains the warm air in it.

Finally, and with respect to the cabin geometry comparison shown in Figure 8, it can be observed that, although the 3 cabins have similar general behaviour, some noticeable differences are present. All of them show to be effective in terms of temperature gradient, as well as having its optimal performance around $\dot{m}_{in} = 20\, g\, s^{-1}\, pax^{-1}$. However, Cabin 2 and 3 show better thermal comfort parameters than Cabin 1 at this optimal inflow rate. It is also noticeable that, although Cabin 2 has similar behaviour than Cabin 3, it only happens for a narrow range of $15\, g\, s^{-1}\, pax^{-1} \geq \dot{m}_{in} \geq 25\, g\, s^{-1}\, pax^{-1}$, being the performance of Cabin 3 more consistent for a wider range of inflow values. In terms of draught, both Cabin 2 and 3 show a drop of DR for their optimal point, and also Cabin 3 shows lower DR values for high mass inlet compared with the other two cabins. Be also noted that they all work well in getting uniform temperature distribution, as it can be concluded from the PDver parameter.

5. Conclusions

Based on the results presented, it can be concluded that the present Zonal Model methodology constitutes a flexible, reliable and fast computing tool for having coarse estimations of the flow and temperature distribution inside a cabin, even capturing big scale relevant events like recirculations. This allows computing extensive comparative studies for solid cabin design decision making, attending to passengers' thermal comfort parameters and with a reasonable computational effort.

Secondly, the studies presented in this paper are just an illustrative example of the type of analysis that can be done with this framework, but there are further design parameters that can be studied following the same scheme (e.g. the air inlets direction or the personal ventilation intensity). Additionally, these comparatives have been assessed according to thermal comfort criteria, however, other objective functions can be also implemented for attending to other design criteria (e.g. air renovation, local air stagnation or cooling energy efficiency).

Moreover, the low computation time characteristics of this approach makes it compatible with further developments. On one hand, this method could be the base for developing an automatized morphological optimizator, where the evaluated objective functions can be the input to the morphing tool already implemented. On the other, some boundary conditions here assumed constant can be the interface to a multiphysics solver. One possible example would be to integrate a thermo-regulatory model of a human to the seat blocs, making the passengers active energy sources interactive with the environment.

6. Contact Author Email Address

Mail to: sergi.tarroc@gmail.com

7. Copyright Statement

The authors confirm that they, and/or their company or organization, hold copyright on all of the original material included in this paper. The authors also confirm that they have obtained permission, from the copyright holder of any third-party material included in this paper, to publish it as part of their paper. The authors confirm that they give permission, or have obtained permission from the copyright holder of this paper, for the publication and distribution of this paper as part of the ICAS proceedings or as individual off-prints from the proceedings.

References

[1] Raina A et al. *CFD Study of Different Aircraft Cabin Ventilation Systems on Thermal Comfort and Airborne Contaminant Transport*. Tech. rep. Linköping University, 2020, p. 66.

[2] Guerrero i Almirall A. *Zonal Model for Thermal Comfort Study using a CFD coarse approach*. Tech. rep. Linköpings Universitet, 2020.

[3] ATR. *ATR 42-300 - Aircraft Handling Manual*. 2018.

[4] Bombardier Inc. *Dash 8 Series 100 - Airport Planning Manual*. 1993.

[5] Biancolini M E et al. *Radial Basis Functions Mesh Morphing*. Vol. 1. Springer International Publishing, 2020, pp. 294–308. ISBN: 9783030504335. DOI: 10.1007/978-3-030-50433-5_23.

[6] Embraer S.A. *Embreaer 190 - Airport Planning Manual*. 2021.

[7] Tárraga Prieto J I. *Zonal Model for Thermal Comfort Study using a Power Law Model*. Tech. rep. Linköpings Universitet, 2020.

[8] ISO 7730:2005. “Ergonomics of the thermal environment - Analytical determination and interpretation of thermal comfort using calculation of the PMV and PPD indices and local thermal comfort criteria”. In: *Iso* 2012 (2012). URL: www.iso.org.

[9] Owen S J. "A survey of unstructured mesh generation technology". In: *7th International Meshing Roundtable* (2000). ISSN: 00295981.

[10] Sarrate J. *A brief introduction to Mesh Generation*. Tech. rep. Universitat Politècnica de Catalunya, 2018.

[11] Versteeg H K and Malalasekera W. "Methods for dealing with complex geometries". In: *An Introduction to Computational Fluid Dynamics - The Finite Volume Method*. 2016, pp. 304–342. ISBN: 9780131274983. DOI: 10.24114/eb.v2i2.4393.

[12] Gharbi L, Ghrab-Morcos N, and Roux J J. "ZAER: A Zonal Model for Heat Transfer and Air Flow in Unconditioned Buildings. - An Experimental Validation". In: *International Journal of Ventilation* (2004), pp. 11–20. ISSN: 1473-3315. DOI: 10.1080/14733315.2004.11683899.

[13] Pang L et al. "Optimization of air distribution mode coupled interior design for civil aircraft cabin". In: *Building and Environment* 134.February (2018), pp. 131–145. ISSN: 03601323. DOI: 10.1016/j.buildenv.2018.02.019. URL: https://doi.org/10.1016/j.buildenv.2018.02.019.

[14] Rhie C M and Chow W L. "Numerical study of the turbulent flow past an airfoil with trailing edge separation". In: *AIAA Journal* 21.11 (1983), pp. 1525–1532. ISSN: 00011452. DOI: 10.2514/3.8284.

[15] National Institute of Standards and Technology. *The Initial Graphics Exchange Specification (IGES) Version 5.3*. 1996.

[16] Kärrholm F P. "Rhie-Chow interpolation in OpenFOAM". In: *Numerical Modelling of Diesel Spray Injection, Turbulence Interaction and Combustion*. Chalmers University of Technology, 2008, pp. 71–75. ISBN: 9781742879758.

[17] Darwish M S and Moukalled F H. "Normalized variable and space formulation methodology for high-resolution schemes". In: *Numerical Heat Transfer, Part B: Fundamentals*. Vol. 26. 1. 1994, pp. 79–96. DOI: 10.1080/10407799408914918.

[18] Tarroc Gil S. *A Fractional Step Zonal Model and Unstructured Mesh Generation Framework for Simulating Cabin Flows*. Tech. rep. Linköping University, 2021.

[19] Boukhris Y, Gharbi L, and Ghrab-Morcos N. "Modeling coupled heat transfer and air flow in a partitioned building with a zonal model: Application to the winter thermal comfort". In: *Building Simulation* 2.1 (2009), pp. 67–74. ISSN: 19963599. DOI: 10.1007/S12273-009-9405-8.